7.2 DAMAGE MECHANISM INTERACTIONS AT THE PLASMA-MATERIALS INTERFACE (*An Early Career Award Project*) — C. M. Parish (Oak Ridge National Laboratory)

OBJECTIVE

This work intends to develop the fundamental scientific basis for modelling and predicting the behavior of helium bubbles in refractory materials, to provide support for the science and engineering of the tokamak plasma-facing-material environment.

SUMMARY

This first reporting period of the five-year project has emphasized experimental technique developments as the necessary foundation for all later work, and has begun several valuable collaborations with other institutions. Specifically, tungsten high-purity sheet stock has been obtained and characterized to act as a constant and known baseline for further experiments. Focused ion beam (FIB) methods to prepare samples for transmission electron microscopy (TEM) of plasma-exposed tungsten have been refined. This includes tall (>1000 nm) "nanofuzz" tendrils, which is a significant experimental challenge. A non-FIB technique for nanotendrils has also been developed. Collaborations thus far include UCSD PISCES laboratory, and Dr. D. Donovan, UT-Knoxville.

PROGRESS AND STATUS

Introduction

As the choice for the ITER divertor, and present leading candidate for subsequent tokamak systems, tungsten metal is the current focus for high-flux, high-fluence, high-temperature plasma-materials interactions (PMI) studies. Unfortunately, the fundamental scientific basis for explaining observed PMI behaviors (e.g., nanofuzz growth) and predicting long-term behaviors (e.g., PMI response in a nuclear environment) is lacking. In this reporting period, we have begun examining defect-defect interactions in tungsten metal that has been subjected to plasma exposure.

Experimental Procedure

In this summary, data from two separate sets of specimens are presented. First is a lower-flux exposed ALMT ITER-grade tungsten blank (Sandia-California system, ~1300 K, 75 eV ion energy, ~2×10^{19} ions/m^{2}sec, ~3×10^{24} ions/m^2 total), the second a high-flux nanotendril coated specimen (UCSD-PISCES, ~1200 K, 50 eV ion energy, ~10^{23} ions/m^{2}sec, ~4×10^{26} ions/m^2 total).

FIB sample preparation has been generally successful using standard methods; the ORNL LAMDA lab FEI Versa DualBeam instrument was used for all results in this report. Samples were milled with 30, 16, 8, and 5 keV Ga^+ beams. Most samples were cleaned post-FIB using the Fishione Nanomill, 900 eV Ar^+ beam, for several minutes on each side to remove Ga contamination and reduce the injected black-spot contrast arising from FIB damage. Samples were also typically cleaned using a $25O_2$-75Ar plasma to reduce carbonaceous contamination in-TEM.

Significant artifacts are introduced in FIB preparation of nanotendrils, such as coating the tendrils with a C-Ga-Pt layer from FIB preparation, so a method to extract individual nanotentrils for TEM was developed. Specifically, 3 mm copper-mesh TEM grids, with either lacy or continuous carbon films, are wet with methanol, grasped with tweezers, and the swabbed across the tendril-coated surface (also wet lightly with methanol). This extracts both bundles of nanotendrils and isolated nanotendrils suitable for individual TEM examination.

Results

The most important PMI-modified microstructural parameter in terms of influence on properties (fuel retention, thermal conductivity, etc.) is the density and size of helium bubbles. Three sample regions are shown in Figure 1; Figure 1a, the low-flux sample's near-surface region; Figure 1b, the nanotendril-coated sample's substrate region (near the substrate/tendril interface); and Figure 1c, the nanotendrils themselves.

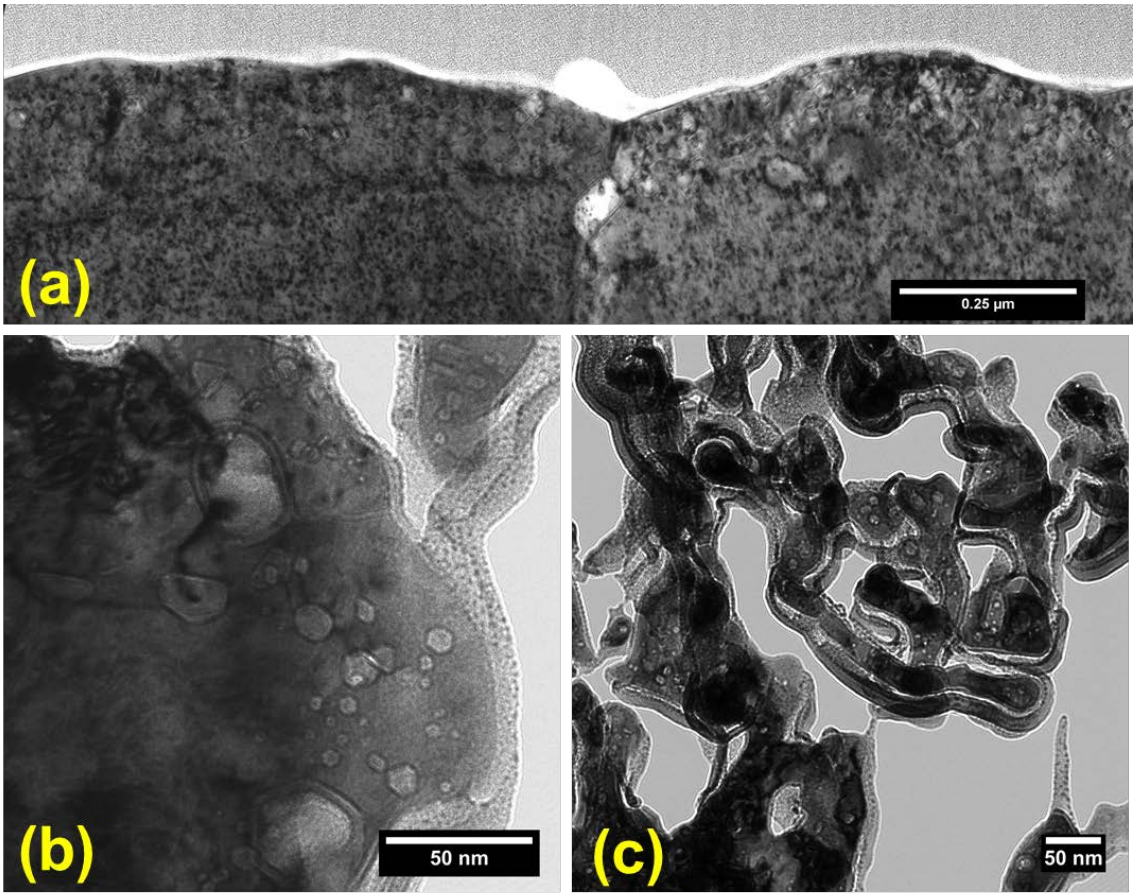

Figure 1. (a) low-flux ALMT-ITER grade specimen, near-surface region. (b) PISCES nanotendril-coated sample, substrate region. (c) PISCES nanotendril-coated sample, tendril region. All three images from FIB-prepared regions.

Analysis of these (and similar) images indicates much larger bubbles in the low-flux, low-fluence specimen compared to nanotendril sample's two regions. Specifically, Figure 1a show mean bubble diameter 16.5 nm with a range from 5-100 nm; Figure 1b, a mean of 7.3 nm with a range of 2-40 nm; and Figure 1c (the tendrils), a mean of 5.9 nm with a range of 3-12 nm.

Although the higher flux and fluence needed to form tendrils might lead to the hypothesis that the bubbles should be larger, this was not observed. One possible mechanism is that as the surface is consumed in order to lengthen the tendrils, the near-surface bubble population is also consumed and new bubbles must be continuously formed, leading to smaller sizes due to shorter lifetimes. Regardless, flux-resolved and interrupted experiments are planned for the near future to begin addressing these questions.

Isolated tendrils, prepared by the method developed recently, are shown in Figure 2a. This new and reliable sample preparation method will allow us to address questions such as grain-boundary character in the tendrils, and might allow EELS-based measurement of the helium content in the bubbles. A convergent-beam electron diffraction pattern is shown in Figure 2b, obtained from the arrowed point in Figure 2a. By analyzing multiple patterns, we intend to determine the grain-to-grain orientation relationships in the tendrils. This should allow inference of growth mechanics (i.e., high-vs-low angle grain boundaries requiring different nucleation energies), as well as providing insight into the energetics of near-boundary bubbles (i.e., Figure 2c). Figure 2d is an EELS low-loss log-ratio thickness map; further technique development for EELS mapping of the energy region of interest to He is underway, in order to gauge the feasibility of direct measurements of He in W.

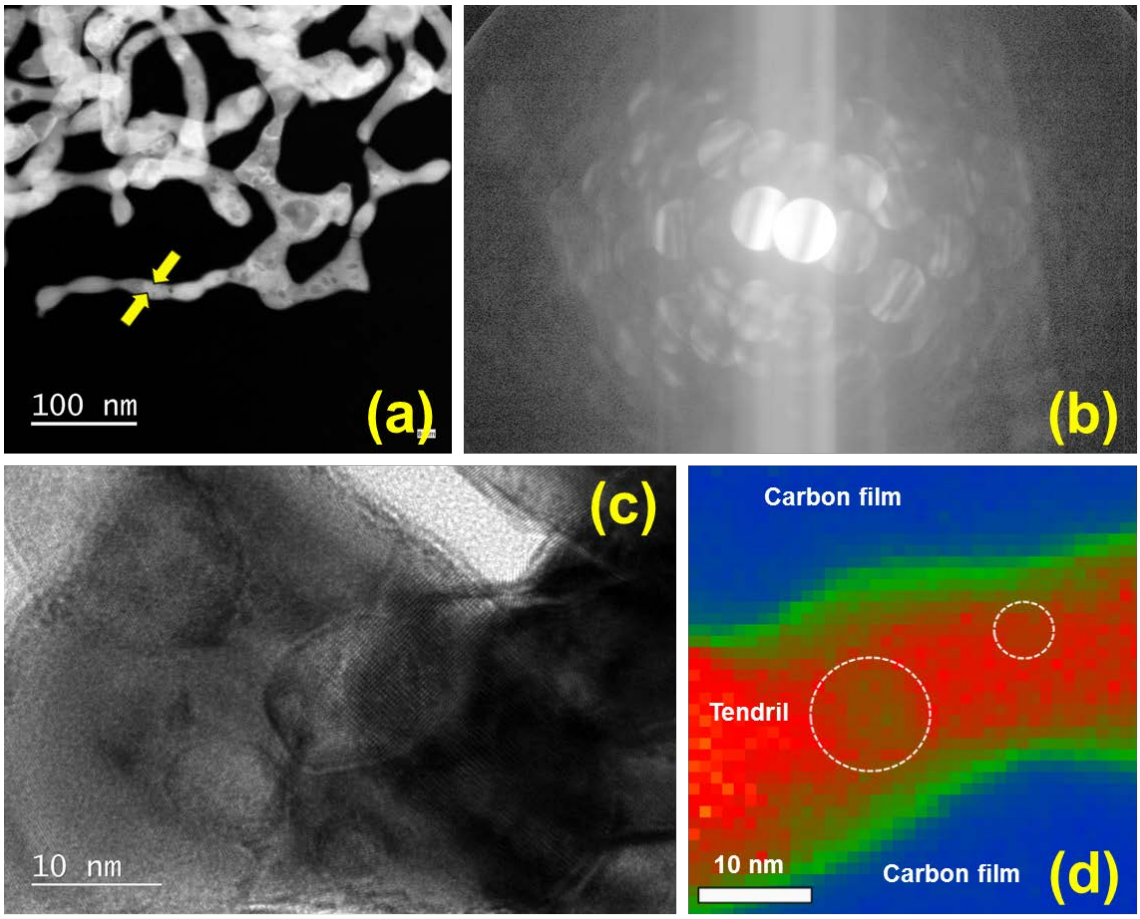

Figure 2. (a) HAADF-STEM image of suspended nanotendrils. (b) Diffraction pattern from arrowed point in (a). (c) High-resolution TEM image of bubbles near boundaries in isolated tendrils. (d) EELS thickness map of a single tendril on the carbon support film. Dashed circles indicate larger bubbles.

The work in this reporting period illustrates a strong basis for ongoing experiments in upcoming reporting periods. With the plasma-exposure experiments planned at collaborator laboratories, flux-resolved and energy-resolved tests of tungsten under helium bombardment will be performed and detailed microstructural parameters will be determined by the methods described here.

Acknowledgements

D .Donovan, UT-Knoxville, and M. Baldwin and R. Doerner, UC-San Diego, provided samples. Talos F200X STEM instrument provided by the Department of Energy, Office of Nuclear Energy, Fuel Cycle R&D Program and the Nuclear Science User Facilities.